Research Article | Vol. 29, No. 2 / 18 January 2021 / Optics Express 2270
Optics EXPRESS

Multi-IF-over-fiber transmission using a commercial TOSA for analog fronthaul networks aiming beyond 5G

SHOTA ISHIMURA,* HSUAN-YUN KAO, KAZUKI TANAKA, KOSUKE NISHIMURA, RYO INOHARA, AND MASATOSHI SUZUKI

KDDI Research, Inc., 2-1-15 Ohara, Fujimino, Saitama 356-8502, Japan
sh-ishimura@kddi-research.jp

Abstract: An IF-over-fiber (IFoF)-based analog transport technology for mobile fronthaul applications has recently attracted significant attention. However, most previous studies have employed discrete optical components. For the analog transport technology to be a more cost-effective and power-efficient solution, it is necessary to utilize existing integrated optical transceivers. In this paper, we demonstrate IFoF transmission using a commercial off-the-shelf transmitter optical sub-assembly (TOSA). Although the TOSA was developed for a digital system employing non-return-to-zero (NRZ) signals, we show that it is also possible for the TOSA to support high-capacity analog transmission. As a demonstration, by using the TOSA, we could successfully transmit 64- and 256-ary quadrature-amplitude-modulated (64/256QAM) orthogonal-frequency-division-multiplexed (OFDM) signals with net bit rates of 54.74 and 36.49 Gbps per wavelength, respectively. Since the TOSA has four wavelength channels, the total capacities are 218.94 and 145.98 Gbps, respectively. To the best of our knowledge, these rates are the highest among all the demonstrations using analog transport technology.

© 2021 Optical Society of America under the terms of the OSA Open Access Publishing Agreement

1. Introduction

Due to the recent development of network-driven applications, such as cloud computing and augmented-reality and virtual-reality (AR/VR) technologies, the total amount of mobile traffic has been growing exponentially. Therefore, such tremendous traffic growth needs to be supported by adopting the high-capacity and low-latency fifth-generation (5G) mobile system. In particular, this data increase puts a burden on mobile fronthaul networks that use digital fiber-optic interfaces (e.g., CPRI) [1]. This is because digital fronthaul interfaces have a much higher data rate than the original throughput [2]. Thus, it is essential to accommodate such substantial traffic using more spectrally-efficient interfaces.

For this purpose, an IF-over-fiber (IFoF)-based analog transport technology for mobile fronthaul applications has recently attracted significant attention. Moreover, numerous demonstrations have shown that the IFoF-based mobile fronthaul network can easily support a CPRI-equivalent capacity as high as several hundred Gbps. However, most authors have used expensive Mach-Zehnder modulators (MZMs) to demonstrate such high-capacity transmission. On the other hand, Ref. [3] showed the applicability of directly-modulated lasers (DMLs) and electro-absorption modulated lasers (EMLs) for cost-effective deployment of analog fronthaul links. Reference [3] demonstrated DML/EML-based transmission using discrete laboratory equipment. The authors concluded that it is possible to realize DML/EML-based analog links without many technical difficulties. However, it is still desired to utilize more compact and less power-consuming integrated DML/EMLs rather than discrete components. Such integrated DML/EMLs have been developed mainly for high-speed Ethernet applications (e.g., 100GbE [4] and 400GbE [5]). We note that the price of high-speed transceivers should go down because the evolution of mega data centers has boosted the demand for them, and thus the sales volume has been increasing [6].

#414714 https://doi.org/10.1364/OE.414714
Journal © 2021 Received 10 Nov 2020; revised 23 Dec 2020; accepted 28 Dec 2020; published 13 Jan 2021

Optics EXPRESS

Therefore, we can implement high-capacity IFoF-based analog mobile fronthaul networks that are cost-effective and power-efficient by utilizing the existing low-cost optical transceivers.

In this paper, we demonstrate IFoF transmission using a commercial off-the-shelf transmitter optical sub-assembly (TOSA) module. Although the TOSA was developed for a digital system employing 4×25 Gbps non-return-to-zero (NRZ) signals, we show that it is also possible for the TOSA to support high-capacity analog transmission. In Ref. [7], we have already reported on IFoF transmission using the TOSA. By extending Ref. [7], this paper describes TOSA characterization and transmission performance in detail. In addition, as a demonstration, we could transmit 64- and 256-ary quadrature-amplitude-modulated (64/256QAM) signals with net bit rates of 54.74 and 36.49 Gbps per wavelength, respectively. Since the TOSA has four wavelength channels, the total capacities are 218.94 and 145.98 Gbps, respectively. which are higher than the capacity reported in Ref. [7]. Although an extremely high capacity of a 5.210-Tb/s CPRI-equivalent data rate was demonstrated using digital radio-over-fiber (D-RoF) technology [8], these bit rates are the highest among all the demonstrations using analog technology reported so far, to the best of our knowledge. The results indicate that IFoF technology can support high-capacity, cost-effective, and power-efficient mobile fronthaul networks by exploiting existing integrated optical transceivers.

2. Experiment

2.1. TOSA characterization

Figure 1(a) shows the external appearance of the TOSA, which was developed for IEEE 100GBASE-ER4 QSFP28 applications. (This TOSA was produced by Mitsubishi Electric.) One lane supports 25 Gbps. The TOSA consists of four individual EML lanes, built-in spatial optical isolators, and filters. The wavelengths of the EMLs are 1295.56, 1300.05, 1304.58, and 1309.14 nm, which follows the LAN-WDM wavelength grid. We note that the use of the O-band is a typical solution for such high-speed transceivers, and there are already a lot of commercial products based on the O-band. Therefore, we can also utilize such O-band solutions for analog systems. Additionally, although the C-band has lower-loss characteristics, the O-band is still attractive since we can operate analog systems in a dispersion-free region.

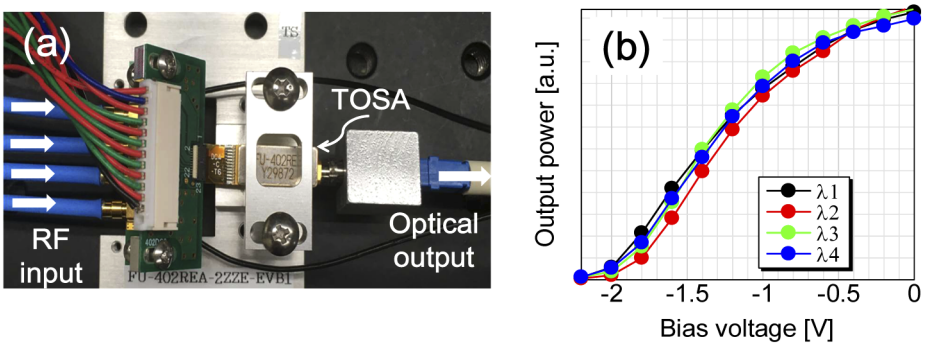

Fig. 1. External appearance of the TOSA (a), and its transfer function (b).

We characterized their transfer curves, as shown in Fig. 1(b). We biased all the EMLs at 100 mA in this measurement. It was found that the center of the curve comes around at −1.25 V. Therefore, we set reverse bias voltages at −1.25V in the following experiments. Note that since analog transmission systems require linear modulation, an electrical input signal to the EML needs to be operated within the linear region (from −1V to −1.5V.) Therefore, the actual peak-to-peak voltage to drive the EML was 0.5 Vpp.

Optics EXPRESS

We also measured the frequency response of the TOSA, as shown in Fig. 2. In the measurement, the optical output from each lane was detected using a 50-GHz PD. Note that the measured response of the TOSA had a small dip in the low-frequency side. This is because the response of the PD itself had the dip. As shown in Fig. 2, the 3-dB bandwidths were observed to be around 20 GHz. Since the TOSA supports a 25-Gbps per lane, the measured 3-dB bandwidth is a reasonable value. As will be discussed later, since the bandwidths of analog signals were < 12 GHz, the 3-dB bandwidth was sufficient for such analog signals.

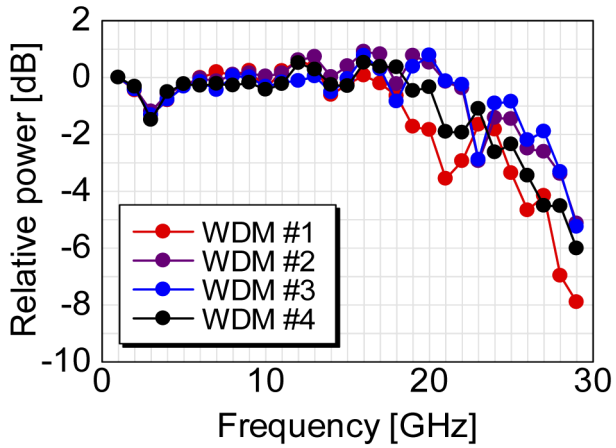

Fig. 2. Frequency response of the TOSA.

2.2. IFoF transmission experiments

We demonstrate IFoF transmission using the TOSA. The experimental setup is depicted in Fig. 3. We tested two modulation formats in this experiment: 64QAM and 256QAM. In the case of 64QAM, we first generated 24 380.16-MHz orthogonal-frequency-division-multiplexed (OFDM) signals using a Keysight 5G NR waveform generator. Each signal had a subcarrier spacing of 120 kHz, and the FFT size and the number of subcarriers were set to be 4096 and 3168, respectively. All these parameters followed the specifications defined for the 5G frequency range 2 (FR2) [9].

Subsequently, we aggregated them in an IF band with a fixed interval of 400 MHz. We also set a guardband from a direct current (DC) component at 100 MHz. Due to the bandwidth limitation of a 5G NR analyzer used on the receiver side, we could not directly inject all 24 channels into the analyzer simultaneously. Therefore, we had to split the signal into several bands. For this purpose, we split the signal into four bands (#1-6, #7-12, #13-18, and #19-24). A band to be measured was extracted using a band-pass filter (BPF) and down-converted to a low-frequency region. Since such an analog filtering process required additional guard bands between the bands, we set fixed guard bands of 600 MHz. Therefore, the total bandwidth of the aggregated signal was around 11.5 GHz. On the other hand, in the case of 256QAM, we aggregated 12 380.16-MHz OFDM signals in an IF band with a fixed interval of 400 MHz. Since the analyzer's bandwidth was sufficient for the signal, we could simply aggregate and directly analyze the 12 channels without an analog filtering process. Consequently, the total bandwidth of the signal became 4.9 GHz. The generated signal was amplified by an RF amplifier, combined with a reverse bias voltage using a bias tee, and injected into the TOSA module. The temperature of the module was maintained at 55°C during the experiment. After being modulated by the EML, the optical signal was transmitted over a single-mode fiber (SMF). Note that the fiber loss at 1.3 μm was around 0.33 dB/km.

Optics EXPRESS

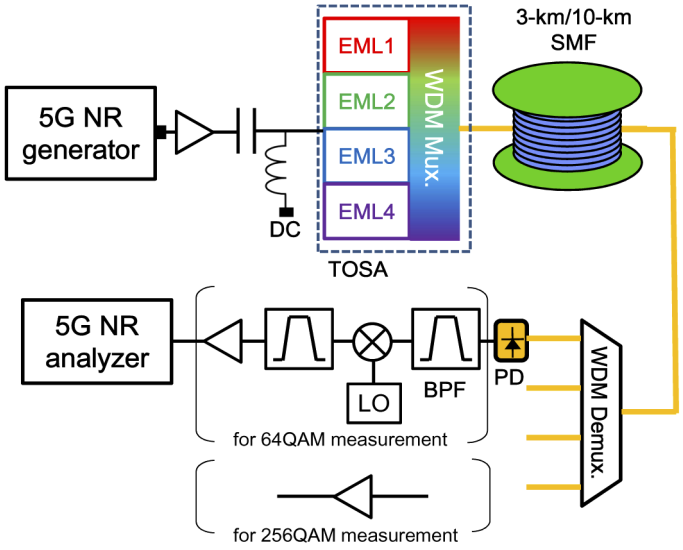

Fig. 3. Experimental setup.

On the receiver side, each WDM channel was extracted using a WDM filter, and the extracted optical signal was detected by a PIN photodiode (PD) with a linear transimpedance amplifier (TIA). The bandwidths of the PD and TIA were 20 GHz, which was sufficient for the analog signals. For the 64QAM case, band selection was performed using a BPF. The selected signal was then down-converted to a low-frequency region so that the 5G NR analyzer could detect it, as explained earlier. On the other hand, for the 256QAM case, the electrical signal was directly captured by the 5G NR analyzer. Finally, we measured the error-vector-magnitude (EVM) performance of each WDM channel one by one.

3. Results and discussion

Figure 4 shows the results for the 64QAM case. The solid and dotted lines show the back-to-back (B2B) case and the case after the 10-km transmission, respectively. First, we measured EVM values by varying received optical power. Figures 4(a), (b), (c), and (d) show EVM values for the WDM channel 1, 2, 3, and 4, respectively, and the red and blue curves show the EVM values for the first and last (24th) channel, respectively. We found that at a minimum received optical power of > -5 dBm was necessary to satisfy the 8% EVM requirement for 64QAM. Since the launched optical power of each WDM channel was around 1-2 dBm, the system margin is estimated to be around 6-7 dB. We should note that this margin can be further improved by employing optical amplifiers such as semiconductor optical amplifiers (SOAs) or avalanche PDs (APDs) on the receiver side. Since some vendors provide receiver optical sub-assembly (ROSA) modules integrated with APDs as off-the-shelf products, we can extend the margin by utilizing such commercial ROSA modules. Next, we show the EVM values for all 24 channels in both the B2B case and the case after 10 km transmission in Figs. 5(a) and (b), respectively, with insets showing the constellations. The received optical power in the B2B state was 0 dBm, while that after the 10-km transmission was around -3 dBm. It can be seen from the figures that the EVM values in both cases could be less than the threshold. Note that we performed pre-emphasis to flatten the frequency response. However, due to the mixer's performance, we still had band-dependent EVM fluctuation, especially on the second band, even after performing pre-emphasis. In addition, each WDM channel had a different frequency response. In fact, there

Optics EXPRESS

was a variation of the EVM values on the first channel from 4.8% to 5.3%, as shown in Fig. 5(a). This resulted in the variation of the blue curves in Fig. 4. On the other hand, we had a larger variation in the last channel, as shown in Fig. 5(a). Due to this relatively large variation, the red curves in Fig. 4 also varied. It should also be noted that we performed pre-emphasis only based on the EVM performance in the B2B state. Since the TOSA was operated in the O-band, we had a negligible dispersion effect, and fiber transmission does not affect the frequency response. Therefore, we did not need to perform pre-emphasis for each transmission distance. If there is distance dependence on frequency response, a specific feedback algorithm may be necessary, which increases the system complexity. Since the use of the O-band eliminates such a necessity as well as the dispersion compensation process, it has the potential to simplify the entire fronthaul systems.

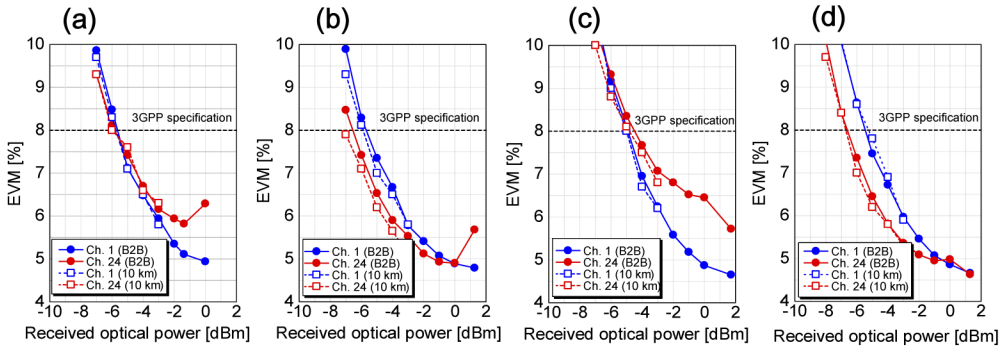

Fig. 4. Experimental results for the 64QAM case. (a), (b), (c), and (d) show the EVMs versus received optical power in the first, second, third, and fourth WDM channels, respectively. The solid and dotted lines show the B2B case and the case after the 10-km transmission, respectively.

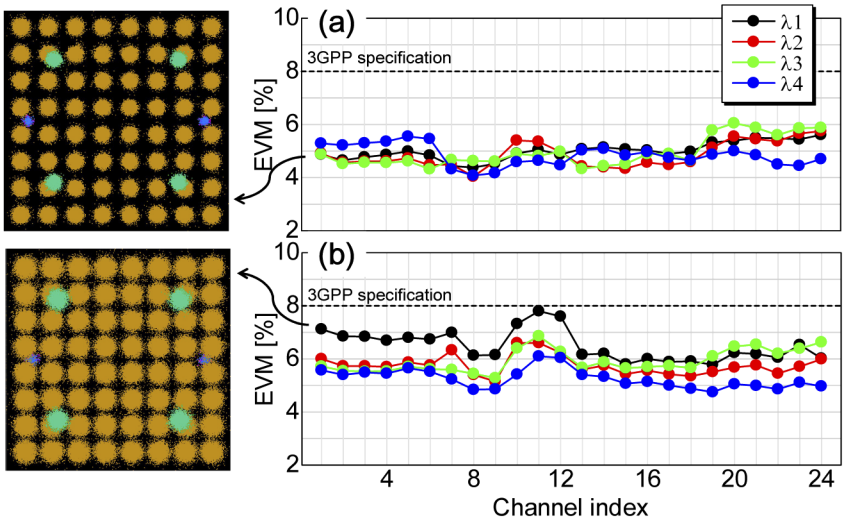

Fig. 5. Experimental results for the 64QAM case. (a) and (b) show EVMs of all the IF channels in the B2B and 10-km cases, respectively, with insets showing the constellations.

Figure 6(a) shows the electrical spectra of the first WDM channel in the B2B case and the case after the 10-km transmission, respectively. In this experiment, we achieved a total net bit rate of

Optics EXPRESS

218.94 Gbps: 4(WDM channel) × 24 (IF channel) × 380.16 MHz × 6 bit/s/Hz. We should note that this capacity is twice as high as the original 100GbE capacity. If these signals are transmitted by CPRI, the corresponding CPRI rate is calculated as 4 (WDM channel) × 24 (IF channel) × 2 (IQ) × 491.52 MHz (sampling rate) × 15 (resolution) × 16/15 (CPRI overhead) × 10/8 (8b/10b encoding) = 1.88 Tb/s. Note that the sampling rate is calculated as follows: the subcarrier spacing and the FFT size were set to be 120 kHz and 4096, respectively, as explained above. Therefore, the baseband sampling rate is 120 kHz × 4096 = 491.52 MHz [9]. It should also be noted that we assume the use of the 8B/10B encoding here, although the 64B/66B encoding is typically employed in high-speed interfaces. So far, most of the papers demonstrating analog RoF transmission assume the 8B/10B encoding in calculating CPRI-equivalent rates. Therefore, we also assume the 8B/10B encoding here to keep the consistency and make a fair comparison.

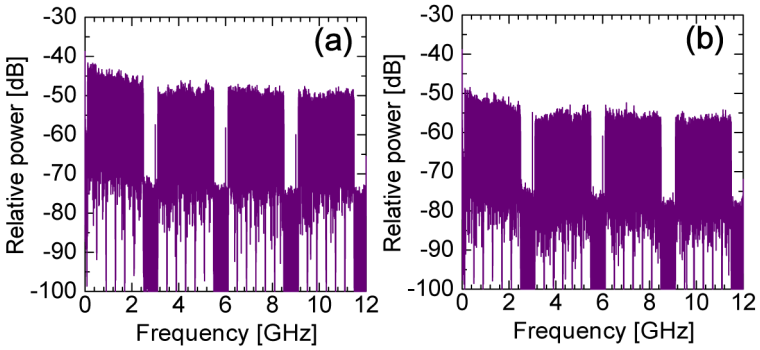

Fig. 6. Electrical spectra of the first WDM channel for the 64QAM case in the B2B state (a) and the case after the 10-km transmission (b).

Next, we show the results for the 256QAM case in Figs. 7 and 8. Figure 7 shows the EVM values in the B2B state. The solid and dotted lines show the B2B case and the case after the 3-km transmission, respectively. As can be seen in Figs. 7(a)-(d), received optical power needs to be larger than −2 dBm to satisfy the 3.5% EVM requirement for 256QAM. Therefore, the margin is estimated to be 3-4 dB. Due to this relatively small margin, we could transmit the signal only over 3 km. Figures 8(a) and (b) show the EVM values for all the 12 channels in both the B2B case and the case after 3-km transmission with insets showing the constellations. The received optical power in the B2B state was 0 dBm, while that after the 3-km transmission was around −1.5 dBm. Since the EVM performance was directly analyzed without analog filtering and down-conversion processing, the EVM curves could be flattened. As can be seen in the figures, all the channels could satisfy the 256QAM criteria. Figures 9(a) and (b) show the electrical spectr of the first WDM channel in the B2B case and the case after the 3-km tranmision, respectively. In this case, we achieved a total net bit rate of 145.98 Gbps: 4(WDM channel) × 12 (IF channel) × 380.16 MHz × 8 bit/s/Hz. The corresponding CPRI rate is calculated as 4 (WDM channel) × 12 (IF channel) × 2 (IQ) × 491.52 MHz (sampling rate) × 15 (resolution) × 16/15 (CPRI overhead) × 10/8 (8b/10b encoding) = 0.94 Tb/s.

Table 1 compares our results with those from other studies [10–26]. As shown in the table, [22] demonstrated 64QAM-based transmission with the widest bandwidth of 22.68 GHz. In this study, we successfully increased the bandwidth 1.6-fold, although we utilized four wavelengths. On the other hand, there have been few reports on 256QAM transmission. So far, [26] demonstrated 256QAM transmission with the widest bandwidth of 12.8 GHz using Gaussian dithering. In comparison with our results, we could further extend the bandwidth by 1.4 times.

Optics EXPRESS

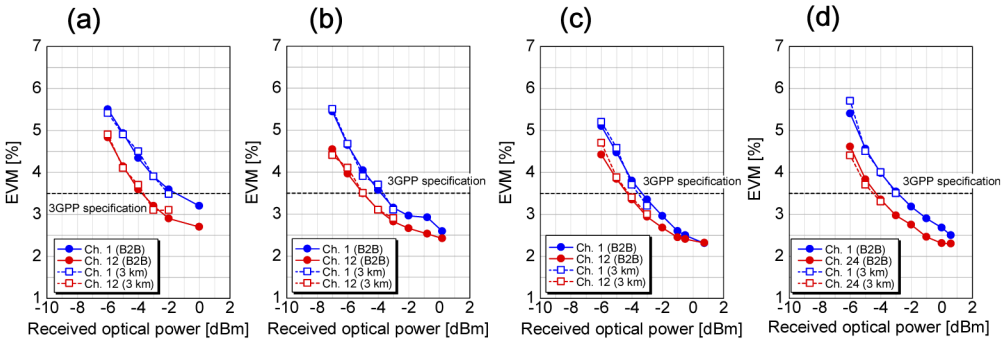

Fig. 7. Experimental results for the 256QAM case. (a), (b), (c), and (d) show the EVMs versus received optical power in the first, second, third, and fourth WDM channels, respectively. The solid and dotted lines show the B2B case and the case after the 3-km transmission, respectively.

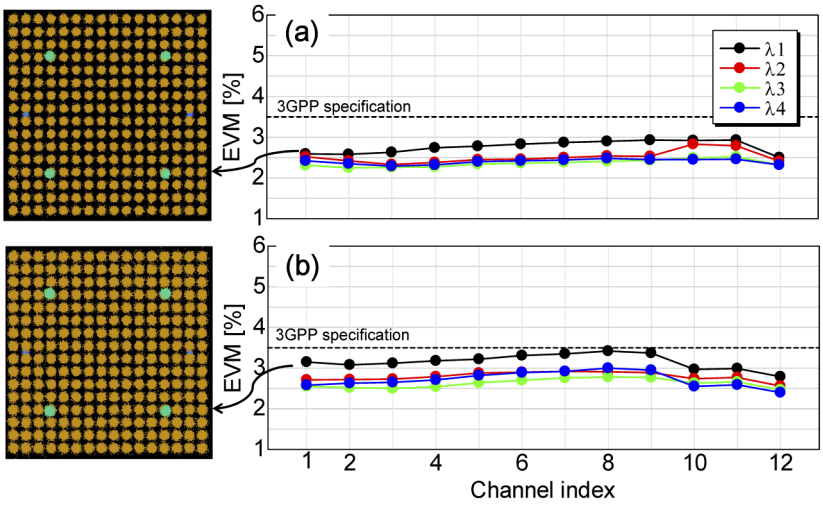

Fig. 8. Experimental results for the 256QAM case. (a) and (b) show EVMs of all the IF channels in the B2B and 3-km cases, respectively.

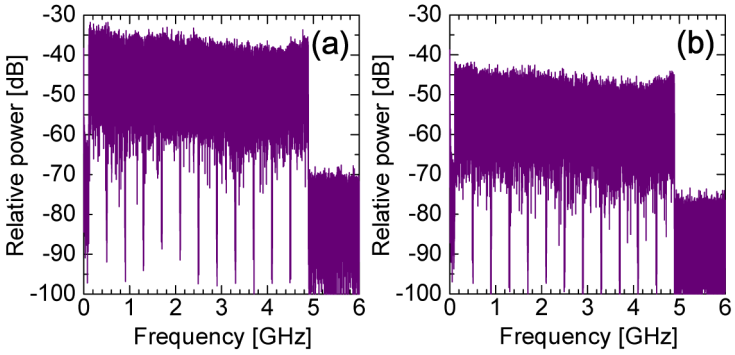

Fig. 9. Electrical spectra of the first WDM channel for the 256QAM case in the B2B state (a) and the case after the 3-km transmission (b).

Optics EXPRESS

Table 1. Comparison of previous reports on IFoF transmission. 1

	Signal BW				Net bit rate [Gbps]	Modulation format	Technical remarks
	λ	IF	BW [GHz]	Total [GHz]			
[10]	1	6	1	6	24	16QAM	V-band transmission
[11]	1	10	1	10	25/40	16QAM/ 32QAM	Bidirectional W-band transmission
[12]	4	1	0.33	1.32	4	16QAM	Si3N4/SiO2 Add/Drop Multiplexer/360° Coverage
[13]	1	12	0.4	4.8	15.6	QPSK/ 16QAM/ 64QAM	Bit/power loading
[14]	1	8	0.1	0.8	4.8	64QAM	5G trial
[15]	1	1	1	1	6	64QAM	Self-steering beamformer
[16]	4	5	0.02	0.1	0.6	64QAM	4 × 4 hand-made optical transceiver
[17]	1	12	0.211	2.532	15.192	64QAM	3s-DBR laser
[18]	1	12	0.5	6	36	64QAM	Blind linearization
[19]	1	32	0.2	6.4	38.4	64QAM	DSP-based aggregation
[20]	1	14	1.2	16.8	100.8	64QAM	Parallel transmitter
[21]	1	14	1.2	16.8	100.8	64QAM	DP-MZM
[22]	1	24	0.945	22.68	136.08	64QAM	KK receiver
[23]	1	7	0.02	0.14	1.04	16QAM/ 64QAM/ 256QAM	Monolithically integrated multi-wavelength transmitter
[24]	1	12	0.198	2.376	19	256QAM	Nonlinear compensation
[25]	1	8	0.6	4.8	38.4	256QAM	SSBI-free PM system
[26]	4	32	0.1	12.8	102.4	256QAM	Gaussian dithering
[7]	4	10	0.38	15.2	121.6	256QAM	Commercial TOSA
This work	4	24	0.38	36.49	218.94	64QAM	Commercial TOSA
	4	12	0.38	18.24	145.98	256QAM	

4. Conclusion

We have demonstrated IFoF transmission using a commercial TOSA. We successfully transmitted 24 64QAM and 12 256QAM 380.16-MHz OFDM signals with net bit rates of 218.94 and 145.98 Gbps, respectively. The corresponding CPRI-equivalent capacities are 1.88 and 0.94 Tb/s, respectively. To the best of our knowledge, these bit rates are the highest among all the analog-based demonstrations reported so far. This study shows the feasibility of IFoF technology utilizing existing integrated optical transceivers. We believe that it is possible for analog fronthaul networks to be implemented at low cost by exploiting such existing transceivers.

Funding. National Institute of Information and Communications Technology.

Acknowledgments. The authors would like to thank Kenichi Uto, Seiki Nakamura, and Ryota Fujihara of Mitsubishi Electric Corp. for their support in the preparation of measurement equipment. Part of the research results have been achieved by "Research and Development of Optical Access Infrastructure for Accommodating Large Capacity Traffic Toward Beyond-5G Mobile Systems," the Commissioned Research of National Institute of Information and Communications Technology (NICT), JAPAN.

Disclosures. The authors declare no conflicts of interest.

References

1. A. Pizzinat, P. Chanclou, F. Saliou, and T. Diallo, "Things you should know about fronthaul," J. Lightwave Technol. **33**(5), 1077–1083 (2015).
2. M. Suzuki, S. Ishimura, K. Tanaka, A. Bekkali, S. Nanba, K. Nishimura, B. G. Kim, H. Kim, and Y. C. Chung, "Optical and wireless integrated technologies for future mobile networks," *Proc. Int. Conf. Transparent Opt. Netw. (ICTON)* pp. 1–4 (2017).
3. B. G. Kim, S. H. Bae, H. Kim, and Y. C. Chung, "RoF-based mobile fronthaul networks implemented by using DML and EML for 5G wireless communication systems," J. Lightwave Technol. **36**(14), 2874–2881 (2018).

Optics EXPRESS

4. T. Murao, N. Yasui, T. Shinada, Y. Imai, K. Nakamura, M. Shimono, H. Kodera, Y. Morita, A. Uchiyama, H. Koyanagi, and H. Aruga, "Integrated spatial optical system for compact 28-Gb/s × 4-lane transmitter optical subassemblies," IEEE Photonics Technol. Lett. **26**(22), 2275–2278 (2014).
5. T. Misawa, S. Yoshimura, T. Saeki, K. Kobayashi, K. Yamaji, D. Shoji, and Y. Fujimura, "High power compact EML transmitter module for 400G-FR4," *Proc. IEEE International Semiconductor Laser Conference (ISLC)* pp. 1–2 (2018).
6. H. Isono, "Latest standardization status and its future directions for high speed optical transceivers," Proc. SPIE **10946**, 1094604 (2019).
7. S. Ishimura, H.-Y. Kao, K. Tanaka, K. Nishimura, and M. Suzuki, "IF-over-fiber transmission of 40×400-MHz 256QAM OFDM signals using commercial 100Gb/s EML TOSA for analog mobile fronthaul networks," *Proc. OptoElectronics and Communications Conference (OECC)* pp. 1–3 (2020).
8. L. Zhang, A. Udalcovs, R. Lin, O. Ozolins, X. Pang, L. Gan, R. Schatz, M. Tang, S. Fu, D. Liu, W. Tong, S. Popov, G. Jacobsen, W. Hu, S. Xiao, and J. Chen, "Toward terabit digital radio over fiber systems: architecture and key technologies," IEEE Commun. Mag. **57**(4), 131–137 (2019).
9. 3GPP TS 138.104 v 15.2.0 release 15, "Base station (BS) radio transmission and reception," 2018.
10. N. Argyris, G. Giannoulis, K. Kanta, N. Iliadis, C. Vagionas, S. Papaioannou, G. Kalfas, D. Apostolopoulos, C. Caillaud, H. Debrégeas, N. Pleros, and H. Avramopoulos, "A 5G mmWave fiber-wireless IFoF analog mobile fronthaul link with up to 24-Gb/s multiband wireless capacity," J. Lightwave Technol. **37**(12), 2883–2891 (2019).
11. P. T. Dat, A. Kanno, N. Yamamoto, N. V. Dien, N. T. Hung, and T. Kawanishi, "Full-duplex transmission of nyquist-scm signal over a seamless bidirectional fiber–wireless system in w-band," *Optical Fiber Communication Conference (OFC)* p. W1I.5 (2019).
12. E. Ruggeri, A. Tsakyridis, C. Vagionas, G. Kalfas, R. M. Oldenbeuving, P. W. L. V. Dijk, C. G. Roeloffzen, Y. Leiba, N. Pleros, and A. Miliou, "A 5G fiber wireless 4Gb/s WDM fronthaul for flexible 360 coverage in V-band massive MIMO small cells," Journal of Lightwave Technology p. early access (2020).
13. M. A. Fernandes, P. A. Loureiro, B. T. Brand ao, A. Lorences-Riesgo, F. P. Guiomar, and P. P. Monteiro, "Multi-carrier 5G-compliant DML-based transmission enhanced by bit and power loading," IEEE Photonics Technol. Lett. **32**(12), 737–740 (2020).
14. M. Sung, J. Kim, E.-S. Kim, S.-H. Cho, Y.-J. Won, B.-C. Lim, S.-Y. Pyun, J. K. Lee, and J. H. Lee, "5G trial services demonstration: IFoF-based distributed antenna system in 28 GHz millimeter-wave supporting Gigabit mobile services," J. Lightwave Technol. **37**(14), 3592–3601 (2019).
15. M.-Y. Huang, Y.-W. Chen, P.-C. Peng, and H. W. andGee Kung Chang, "A full field-of-view self-steering beamformer for 5g mm-wave fiber-wireless mobile fronthaul," J. Lightwave Technol. **38**(6), 1221–1229 (2020).
16. J. Liu, Y. Ye, L. Deng, L. Liu, Z. Li, F. Liu, Y. Zhou, J. Xia, and D. Liu, "Integrated four-channel directly modulated O-band optical transceiver for radio over fiber application," Opt. Express **26**(17), 21490–21500 (2018).
17. Y. Zhu, Y. Wu, H. Xu, C. Browning, L. P. Barry, and Y. Yu, "Experimental demonstration of a WDM-RoF based mobile fronthaul with f-OFDM signals by using directly modulated 3s-DBR laser," J. Lightwave Technol. **37**(16), 3875–3881 (2019).
18. P. Li, W. Pan, L. Huang, X. Zou, Y. Pan, Q. Zhou, Y.-W. Chen, P.-C. Peng, S. Liu, S. Shen, and G.-K. Chang, "Multi-IF-over-fiber based mobile fronthaul with blind linearization and flexible dispersion induced bandwidth penalty mitigation," J. Lightwave Technol. **37**(16), 3875–3881 (2019).
19. X. Liu, H. Zeng, N. Chand, and F. Effenberger, "Efficient mobile fronthaul via DSP-based channel aggregation," J. Lightwave Technol. **34**(6), 1556–1564 (2016).
20. S. Ishimura, A. Bekkali, K. Tanaka, K. Nishimura, and M. Suzuki, "1.032-Tb/s CPRI-equivalent rate IF-over-fiber transmission using a parallel IM/PM transmitter for high-capacity mobile fronthaul links," J. Lightwave Technol. **36**(8), 1478–1484 (2018).
21. A. Bekkali, S. Ishimura, K. Tanaka, K. Nishimura, and M. Suzuki, "High capacity mobile fronthaul using DP-MZM-based IF-over-fiber system with 1-Tbit/s CPRI-equivalent data rate," *Proc. IEEE Int. Conf. Commun. (ICC)* pp. 1–6 (2018).
22. S. T. Le, K. Schuh, M. Chagnon, F. Buchali, and H. Buelow, "1.53-Tbps CPRI-equivalent data rate transmission with the Kramers-Kronig receiver for mobile fronthaul links," *Proc. Eur. Conf. Opt. Commun. (ECOC)* pp. 1–3 (2018).
23. M. S. B. Cunha, E. S. Lima, N. Andriolli, D. H. Spadoti, G. Contestabile, and A. Cerqueira, "5G NR RoF system based on a monolithically integrated multi-wavelength transmitter," IEEE J. Sel. Top. Quantum Electron. **27**(2), 1–8 (2021).
24. B. G. Kim, S. H. Bae, and Y. C. Chung, "Blind compensation technique for nonlinear distortions in RoF-based mobile fronthaul network by using EML," Opt. Fiber Technol. **47**, 51–54 (2019).
25. S. Ishimura, H.-Y. Kao, K. Tanaka, K. Nishimura, and M. Suzuki, "SSBI-free direct-detection system employing phase modulation for analog optical links," J. Lightwave Technol. **38**(9), 2719–2725 (2020).
26. B. G. Kim, S. H. Bae, M. Kim, S. Ishimura, K. Tanaka, K. Nishimura, M. Suzuki, and Y. C. Chung, "Demonstration of reflection-tolerant RoF-based mobile fronthaul network for 5G wireless system," *Proc. Eur. Conf. Opt. Commun. (ECOC)* pp. 1–3 (2019).

209.14.71.2 {ts '2021-12-14 14:22:35'}